

Current Topics in Pathology

Ergebnisse der Pathologie

Edited by

E. Grundmann · W. H. Kirsten
Münster · *Chicago*

Advisory Board

Volume 57



Current Topics in Pathology

Ergebnisse der Pathologie

Edited by

E. Grundmann · W. H. Kirsten

Münster

Chicago

Advisory Board

*H.-W. Altmann, Würzburg · K. Benirschke, La Jolla · A. Boble, Tübingen
K. M. Brinkhous, Chapel Hill · P. Cohrs, Hannover · H. Cottier, Bern
M. Eder, München · P. Gedigk, Bonn · W. Giese, Münster · Chr. Hedinger, Zürich
S. Iijima, Hiroshima · I. Klatzo, Bethesda · K. Lennert, Kiel
H. Meessen, Düsseldorf · W. Sandritter, Freiburg · G. Seifert, Hamburg
H. C. Stoerk, New York · H. U. Zollinger, Basel*

Volume 57

With 80 Figures



Springer-Verlag Berlin · Heidelberg · New York 1973

This work is subject to copyright. All rights are reserved, whether the whole or part of the material is concerned, specifically those of translation, reprinting, re-use of illustrations, broadcasting, reproduction by photocopying machine or similar means, and storage in data banks.

Under § 54 of the German Copyright Law where copies are made for other than private use, a fee is payable to the publisher, the amount of the fee to be determined by agreement with the publisher. © by Springer-Verlag Berlin · Heidelberg 1973. Library of Congress Catalog Card Number 56-49162. Printed in Germany.

The use of registered names, trademarks, etc. in this publication does not imply, even in the absence of a specific statement, that such names are exempt from the relevant protective laws and regulations and therefore free for general use.

Typesetting, printing and binding: Universitätsdruckerei H. Stürtz AG, Würzburg

List of Contributors

SOLANGE G. ABUNASSAR, Beekman Downtown Hospital, 170 William Street,
New York, NY 10037, USA

HENRY A. AZAR, Veterans Administration Hospital, 13000 North 30th Street,
Tampa, FL 33612, USA

J. STEVEN McDUGAL, Columbia-Presbyterian Medical Center, 622-630 West
168th Street, New York, NY 10032, USA

M. MENDELOVICI, Universidad de Los Andes, Apartado 75, Mérida, Venezuela

J. MOPPERT, I. Medizinische Klinik der Universität, Bürgerspital, CH-4000
Basel, Switzerland

EDWARD A. MOSCOVIC, Harlem Hospital Center, 136th Street and Lenox
Avenue, New York, NY 10038, USA

HERWART F. OTTO, Pathologisches Institut der Universität, D-2000 Ham-
burg-20, Martinstraße 52, Germany

HANSPETER ROHR, Pathologisches Institut der Universität, Schönbein-
straße 40, CH-4056 Basel, Switzerland

K. SALFELDER, Instituto de Anatomia Patologica, Universidad de Los Andes,
Apartado 75, Mérida, Venezuela

J. SCHWARZ, Clinical Laboratories, Jewish Hospital, Cincinnati, OH 45229,
USA

G. THIEL, Medizinische Universitätsklinik, Bürgerspital, CH-4000 Basel,
Switzerland

HANS ULRICH ZOLLINGER, Pathologisches Institut der Universität, Schönbein-
straße 40, CH-4056 Basel Switzerland

1.50元
8A
G81

Contents

ZOLLINGER, H. U., MOPPERT, J., THIEL, G., ROHR, H.-P.: Morphology and Pathogenesis of Glomerulopathy in Cadaver Kidney Allografts Treated with Antilymphocyte Globulin (Clinical, Light, Electron and Immunofluorescent Optic Examinations). With 42 Figures	1
AZAR, H. A., MOSCOVIC, E. A., ABUNASSAR, S. G., MCDUGAL, J. S.: Some Aspects of Sarcoidosis. With 14 Figures	49
OTTO, H. F.: The Interepithelial Lymphocytes of the Intestinum. Morphological Observations and Immunological Aspects of Intestinal Enteropathy. With 14 Figures	81
SALFELDER, K., MENDELOVICI, M., SCHWARZ, J.: Multiple Deep Fungus Infections: Personal Observations and a Critical Review of the World Literature. With 10 Figures	123
Author Index	179
Subject Index	195

463.484

10932/3

Morphology and Pathogenesis of Glomerulopathy in Cadaver Kidney Allografts Treated with Antilymphocyte Globulin*

(Clinical, Light, Electron and Immunofluorescent Optic Examinations)

H. U. ZOLLINGER, J. MOPPERT, G. THIEL, H.-P. ROHR

With 42 Figures

Contents

A. Material and Method	1
B. Findings	8
1. Light and Electron Microscopy	8
2. Immuno-Histology	27
3. Clinical Findings	27
C. Discussion	31
D. Summary	42
References	44

Severe glomerular changes occurring in long-surviving kidney transplants have been known for some years. Several authors have interpreted them as glomerulonephritis (lit. cf. HUME *et al.*, 1970, MILGROM *et al.*, 1971). The present paper intends to mainly clarify the light-, electron- and immunofluorescent-optic morphology, and to decide whether it could be glomerulonephritis. Besides, we were interested in the correlation between transplant glomerulopathy (TGP) and clinical findings. Finally, we tried to clarify the pathogenesis of this peculiar TGP and looked for some causal relationship to antilymphocytic globulin (ALG) treatment.

A. Material and Method

21 cases of patients with cadaver kidney transplants were evaluated by 30 kidney punctates and 7 kidney slices. Cases 3 and 19 were examined immediately post mortem; in patients 2, 9, 17, 18 and 21 nephrectomy specimens were at hand. All cases were examined in paraffin (HE, PAS, Picro-Mallory, CAB, Giemsa, methenamine-silver staining) and semithin sections (azur eosin)

* Supported by Swiss National Foundation for Scientific Research No. 3—307.70

by light and electron microscopy: Kidney tissue was split into small tissue blocks, fixed in phosphate-buffered glutardialdehyde (3 %, pH 7,25) and post-fixed in osmium tetroxide (2 %); then embedded in Epon (Epikote 812). Reichert Ultratom OmU2 was used for sectioning. Ultrathin sections were stained with uranyl acetate and lead citrate. A Zeiss electronmicroscope type 9A was available for electron microscopic examination.

The essential changes, etc. are shown in Table 1, whereas the relations between degree of severity, space of time after transplantation and ALG treatment are depicted in Fig. 1.

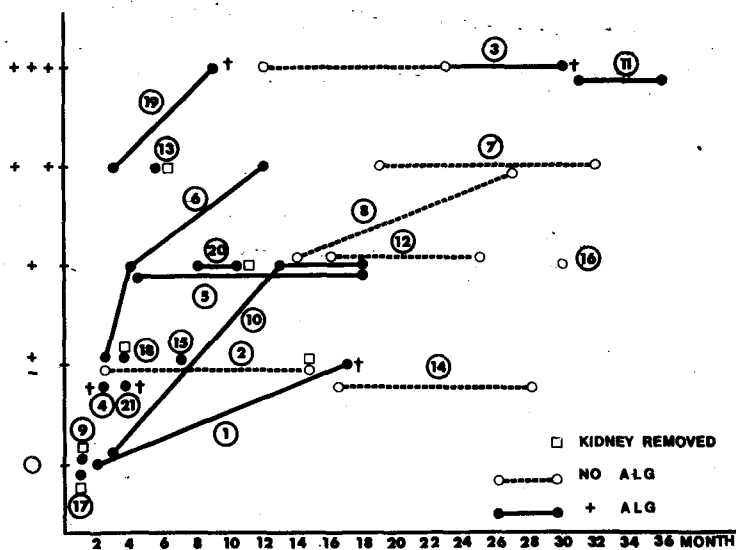


Fig. 1. Relations between grade of severity of transplant glomerulopathy (0 — +++), space of time after transplantation and antilymphocytic globulin (ALG) treatment. Compare case numbers with tables 1 and 2

We examined 32 biopsies of 20 patients by immunofluorescence-histology (s. Table 2). No material was available in case 13 and the first biopsy of cases 1, 2, 3, and 12. Processing: Incubation for 30 min in a moist at room temperature of airdried kryostat sections with rabbit-immune sera (Behring, Germany): 7S specific antihuman IgG-IgM, also antihuman β 1C (C'3), antihuman fibrin and anti-horse-gammaglobulin. After thorough washing of the preparations, second incubation with FITC marked pig-anti-rabbit-gammaglobulin (Sevac, Prague). After repeated washings, evaluation by WILD M 20 microscope by means of blue-light fluorescence. As controls served sections of a normal human kidney which, due to technical reasons, could not be transplanted.

In 12 out of 22 examined cadaver kidney transplants (21 recipients) histocompatibility was tested by means of lymphocyte typing. A modification of Terasaki's method of microcyte toxicity was applied (JEANNET *et al.*, 1969/70).

Table 1. Presentation of cases (for immunohistology see Table 2)

Column 3: Fabry = morbus Fabry, Gl.n. = glomerulonephritis, Py.n. = pyelonephritis, i.n. = non destructive interstitial nephritis, m. G.l.n. = membranous glomerulonephritis, m.n.s. = malignant nephrosclerosis.

Column 4: a = histocompatibility ranks of RAPAPORT and DAUSSET (1969).

b = clinical histocompatibility classification (see text).

Column 5: file number of punch.

Column 6: time since transplantation: d = days, w = weeks, m = months.

Column 7: Creatinine clearance (ml/min.).

Column 8: Antilymphocytic serum therapy: 1 = stop 10 months after transpl., 2 = since 4 months only intramuscularly, 3 = since 10 months only muscularly, 4 = total 40 ml for three days after transpl., 5 = stop 3 1/2 months after transpl., 6 = stop 5 months after transpl., 7 = stop 4 1/2 months after transpl.

Column 9: X-ray treatment.

Column 11: Degree of severity of TGP: Ø = no conspicuous change; ± = slight changes; + = distinct TGP; ++ = rather severe degree of TGP; +++ = extremely severe degree.

Column 12: Osmiophilic deposits: c = capsular BM, s = subendothelial, m = mesangial.

Column 13: d, w, m see column 6; nephrectomy because of: v.r. = vascular rejection, s.r. = spontaneous rupture of transpl. kidney, a.h. = arterial haemorrhage, n.u. = necrosis of ureter, a.r. = acute rejection.

1	2	3	4	5	6	7	8	9	10	11	12	13
Case	Age	Prim. disease	Histocomp. a b	Pct.	Time since transpl.	Ccr.	ALG	Rö.	Prot. uria. mg/die	Glomerulo- pathia	Osmioph. depots	Katamnesis
1	38, ♂	Fabry	— B	276	6 1/2 m	42	Ø	900 R	45	Ø	c +	s. Pct. 400
	38, ♂	Fabry	— B	400	16 1/2 m	8,3	+	900 R	289	±	s + +	† 16 1/2 m: nocardia pneumonia
2	35, ♀	Gl.n.	— C	330	6 w	25	Ø	1200 R	720	±	Ø	s. Pct. 420
	35, ♀	Gl.n.	— C	420	14 m	0	+ ¹	1200 R	8800	±	s +	v. r. 14 m
3	46, ♀	Gl.n.	— B	342	12 m	44	Ø	Ø	598	+ + +	Ø	s. Pct. 490
	46, ♀	Gl.n.	— B	416	23 m	39	Ø	Ø	4450	+ + +	Ø	s. Pct. 490
	46, ♀	Gl.n.	— B	490	30 m	9	+	Ø	2000	+ + +	Ø	† 30 m: liver dystrophy

1	2	3	4	5	6	7	8	9	10	11	12	13	
Case	Age	Prim. Sex	Histocomp.	Pct.	Time since transpl.	Ccr.	ALG	Rö.	Prot. uria mg/die	Glomerulopathia	Osmioph. depots	Katamnesis	
													a Rank
4	29, ♀	Py.n.	8	C	409	50 d.	7.4	+	450 R	1120	±	∅	a.r.: 51 D; † 9 m: influenza p pneumonia
5	24, ♂	i.n.	9	B	422	10 w	40	+	450 R	280	+	∅	functioning
	24, ♂	i.n.	9	B	614	19 m	34	+	450 R	280	+	m+	functioning
6	46, ♀	i.n.	5	B	468	30 d.	8.8	+	450 R	650	±	c+	functioning
	46, ♀	i.n.	5	B	520	6 m	37	+ ²	450 R	150	+	c+	functioning
	46, ♀	i.n.	5	B	597	11 ¹ / ₂ m	26	+ ³	450 R	560	±	∅	functioning
7	27, ♂	Gl.n.	—	A ₂	459	19 m	73	∅	450 R	315	++	s++ m+	functioning
	27, ♂	Gl.n.	—	A ₂	619	32 m	62	∅	450 R	825	++	c+ m++ s++	functioning
8	40, ♂	Gl.n.	—	A ₂	498	14 ¹ / ₂ m	75	+ ⁴	600 R	3100	+	∅	functioning
	40, ♂	Gl.n.	—	A ₂	660	27 m.	72	+ ⁴	600 R	2500	++	∅	functioning
9	47, ♂	Gl.n.	6	C	519	7 d.	0	+	∅	?	∅	m++	v.r. 10 d, sec. transpl.
10	47, ♂	Py.n.	8	B	411	7 w	86	+	750 R	580	∅	∅	functioning
	47, ♂	Py.n.	8	B	522	13 m	50	+	450 R	2900	+	s++	functioning
	47, ♂	Py.n.	8	B	594	18 m	43	+	750 R	4700	+	∅	functioning
11	36, ♀	Gl.n. + diab.	—	B	523	31 m	16	+	∅	780	+++	s+	functioning
	36, ♀	Gl.n. + diab.	—	B	594	36 m	5.4	+	∅	900 —10500	+++	s++	v.r. 49 m, † 49 m thrombocytopenia

12	44, ♀ Gl.n.	—	A ₁	546	16 m	73	0	450 R	216	+	0	functioning
	44, ♀ Gl.n.	—	A ₁	571	25 m	95	0	450 R	460	+	0	functioning
13	45, ♂ m. Gl.n.	—	C	410	5½ m	42	+	300 R	625	++	m++	v.r. 6½ M
14	45, ♂ Gl.n.	—	A ₁	547	16½ m	63	0	450 R	140	±	m+	functioning
	45, ♂ Gl.n.	—	A ₁	604	28 m	64	0	450 R	75	±	m±	functioning
15	34, ♂ i.N.	2	A ₁	566	8 m	97	+ ⁶	0	1080	±	m++	functioning
16	40, ♂ Gl.n.	—	A ₁	581	30 m	85	0	600 R	2000	±	0	functioning
17	46, ♂ Py.n.	4	0	595	8 d	0	+	450 R	?	0	0	s.r. 8 d
18	47, ♂ Gl.n.?	3	0	582	34 d	70	+	0	325	±	0	a.h. 34 d
19	24, ♀ Gl.n.	6	C	605	3½ m	40	+	1050 R	850	++	0	s.Pct. 677
	24, ♀ Gl.n.	6	C	677	9 m	0	+ ⁶	1050 R	?	+++	0	v.r. 9 m † pyocyanus septicemia
20	47, ♀ Py.n.	4	B	611	7 m	57	+ ⁷	750 R	144	+	0	functioning
	47, ♀ Py.n.	4	B	634	9 m	54	+ ⁷	750 R	140	+	0	v.r. 9 m
21	50, ♂ m.n.s.	5	C	635	10 w	0	+	350 R	130	±	0	n.u. 3 m † 4½ m cardiac insufficiency

Table 2. Immunofluorescent findings

IG: Immunoglobulins. C'3: β 1C/1A. Fi: Fibrin(ogen). ALG: Horse antilymphocyte globulin. OSI: Overall severity of immunofluorescent findings *irrespective* of ALG-depositions. Intraglomerular localization: me: mesangial, p: along the periphery of glomerular capillary loops (i.e. basement membrane), mep: combination of me and p., cl: within glomerular capillary lumina.

Pattern of glomerular fluorescence: f: focal, d: diffuse. Amount of fluorescence:

∅ = negative.

+ = less than 30 % of structures positive; slight.

++ = 30—60 % of structures positive; moderate.

+++ = over 60 % of structures positive; marked.

*) = immunofluorescent pattern of nephrotoxic plus complex-type nephritis induced by ALG.

Table 2a:

Case N.	Biopsy N.	IG	C'3	Fi	ALG	OSI
1	276	Immunofluorescent microscopy not done				
1	400	mep f +	p f ++ p d +	mep f +	p f ++ p d +	+
2	330	Immunofluorescent microscopy not done				
2	420	∅	∅	∅	p f ++	∅
3	342	Immunofluorescent microscopy not done				
3	416	mep f ++	mep f ++	mep f +++ ∅		+++
3	490	mep f ++	mep f +	mep f +	mep f ++	+++
4	409	mep f +	∅	mep f +	p d +++	+
5	422	me f +	p d ++	∅	p d +++	+
5	614	me f +	me f +	∅	p d +++	+
6	468	∅	p d +++	∅	p d +++	∅
6	520	∅	∅	∅	p d +++	∅
6	597	∅	∅	∅	p d +++	∅
7	459	mep f ++	mep f ++	∅	∅	++
7	619	mep f ++	mep f ++	me f +	∅	+++
8	498	me f ++	me f +	∅	∅	+
8	660	me f +	me f +	∅	∅	+
9	519	∅	∅	cl f +	p d +++	∅

Initially, 13 HL-A-antigens were tested. Subsequently the number was gradually increased to 24 (JEANNET *et al.*, 1974). According to RAPAPORT and DAUSSET (1970) HL-A-compatibility was assessed in ranks 1–15.

The role of HL-A histocompatibility between non-related donors is controversial. Therefore, in addition, the degree of histocompatibility was retro-

Table 2b:

Case N.	Pct. nr.	IG	Immunofluorescent findings II			
			C'3	Fi	ALG	O _{SI}
10	411	me f ++	∅	me f +	p d +++	+
10	522	∅	∅	∅	p d +++	∅
10	594	p d +++ p f ++	∅	∅	p d +++ p f ++*)	
11	523	mep f ++	mep f ++	mep f +	mep f ++	+++
11	591	mep f ++	mep f ++	cl f +	mep f ++	+++
12	546	Immunofluorescent microscopy not done				
12	571	mep f +	mep f +	∅	∅	+
13	410	Immunofluorescent microscopy not done				
14	547	mep f +	mep f +	mep f +	∅	+
14	604	mep f ++	mep f ++	me f +	∅	+
15	566	∅	∅	∅	p d +++	∅
16	581	mep f ++	mep f +	mep f +	∅	++
17	595	∅	∅	∅	p d +++	∅
18	582	∅	∅	∅	p d +++	∅
19	605	me f ++	me f ++	∅	p d +++ me f ++	++
19	677	mep f ++	mep f ++	∅	mep f ++	++
20	611	me f +	me f +	∅	p d +++	+
20	634	me f +	∅	∅	p d +++	+
21	635	∅	∅	∅	p d +++	∅

spectively rated by the clinical course. 4 ranks of clinical compatibility were distinguished:

O = non-assessable because of a too short course or non-immunologic reasons of failure.

A = good clinical compatibility, i.e. course without any signs of rejection (A_1), or only 1-2 acute rejection episodes easily influenced by therapy without further tendency of relapse (A_2).

B = 1 or more severe rejection episodes which could be brought under control only with difficulties.

C = irreversible acute, subacute or quickly progressing chronic rejection, unaffected by therapy.

All patients were treated with the standard dosage of azothioprine and prednisone. 14 cases additionally received antilymphocytic globulin (ALG) i. v. (THIEL, 1969). In patient 11 azothioprine was stopped 7 months before the first, and 12 months before the second biopsy. During this time, she received only ALG i. v. and a small dosage of prednisone (0-15 mg daily).

The kidney biopsies were chiefly carried out percutaneously with a modified Silverman needle. Proteinuria was measured in the 24-h-urine by Kjeldahl's method of protein analysis; its values were given in mg protein per 24 hs. Table 1 lists the proteinuria of each patient at the time of the kidney biopsy.

B. Findings

1. Light and Electron Microscopy

In light microscopy (Fig. 2) only moderately severe and severe degrees of TGP show an enlarged mesangium and a thickened basement membrane (BM). In semithin sections, the picture of the severe changes reminds of membranous glomerulonephritis (Fig. 3). Silver staining, however, often shows a duplication of the BM; spikes on the external membrane are lacking (Fig. 4). In cases of extremely severe lesions, the loops are often heavily narrowed by the thickened BM. An increase in the number of cells can be demonstrated neither in the mesangium, nor in the endothelium, nor in the capsular epithelium (exception: case 3, s. below).

Glomerular changes, caused by collapse, can regularly be found in cases with severe vascular involvement (cases 1, 2, 4, 9). The BM of the loops is profusely undulated; the loops have collapsed (Fig. 5). Furthermore, these cases show scattered, completely hyalinized glomerula. Mixtures of collapse and TGP were often observed.

Electron microscopy shows the *glomerular basement membrane* thickened in all cases of TGP (Fig. 6). Stronger magnification reveals that the external lamina rara, as well as the lamina densa, ordinarily do not indicate deviation from normal. Only in cases of vascularly triggered collapse of the loops the entire BM is thickened, whereby mainly the lamina densa seems to be enlarged (Fig. 7). — In a very severe grade of TGP it is often difficult to determine the exact boundary between lamina densa and internal lamina rara. The impression, that the lamina densa is distinctly narrowed under these circumstances, is evident (Fig. 8).

The main changes of TGP occur in the internal lamina rara. We observed the first changes in this series of cases after 1½ months (cases 2, 4, 6) (Fig. 1). They consist in finely granular electron-lucent thickenings of the internal lamina rara. In relation to a given loop, the change may be rather diffuse, or nodular (Figs. s. 9-11). Apart from loosely arranged finest osmiophilic granula (Fig. 10, 12, 13, 19, 20), an actual structure of this loosened internal lamina rara can, even at high magnification, not be recognized. In 5 cases, we found osmiophilic filaments in it; this may be fibrin, split or in the process of splitting (Fig. 21).

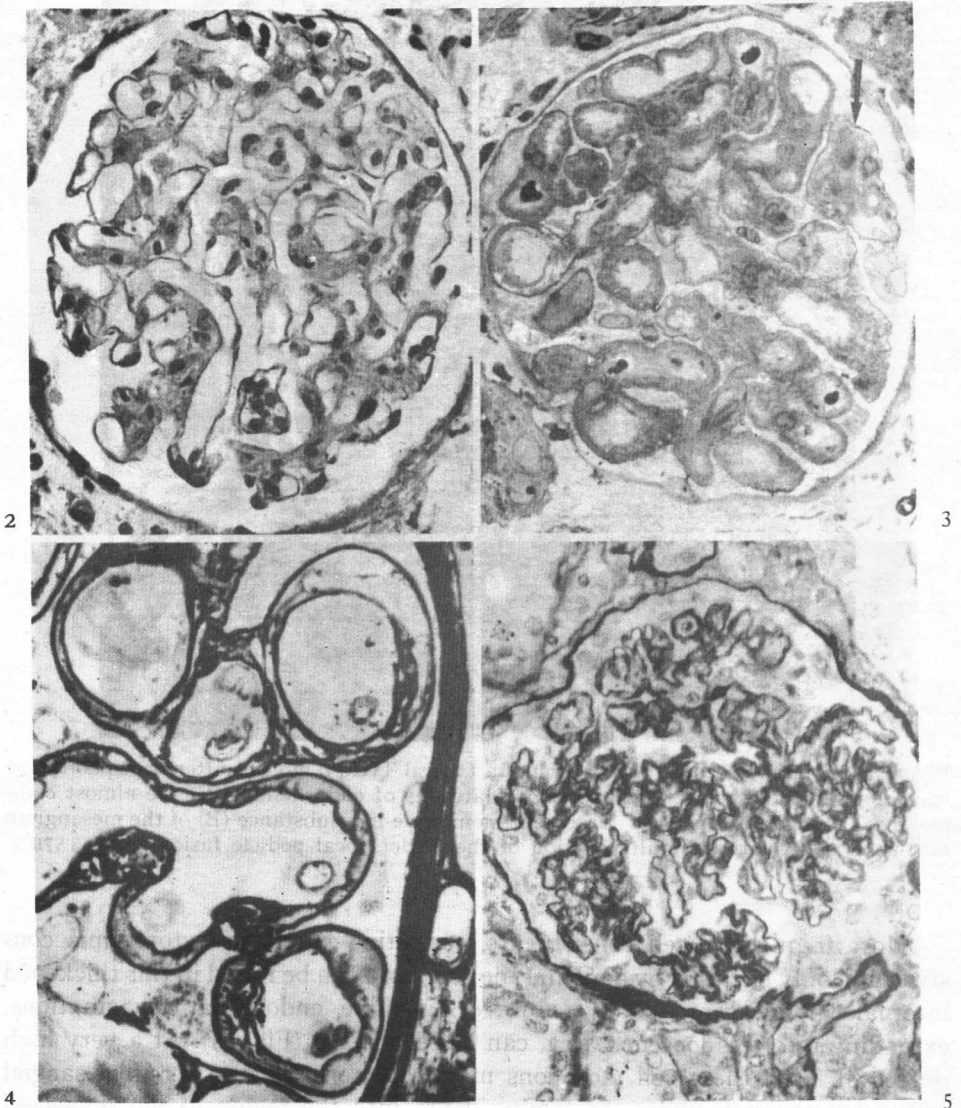


Fig. 2. TGP grade ++, $3\frac{1}{2}$ months after transplantation (case 19). Thickening of the walls of some glomerular loops, increase of mesangial area without nuclear proliferation. PAS, $375\times$

Fig. 3. Very distinct TGP, $2\frac{1}{2}$ years after transplantation (case 11). Greatly thickened capillary walls, no proliferation of cells. One capillary lumen almost blocked (\rightarrow). Semithin section, azur eosin staining, $375\times$

Fig. 4. Same case as Fig. 3, $\frac{1}{2}$ year later (3 years after transpl.). Distinct duplication of the basement membrane, optically empty space between the two layers. Semithin section, methenamine-silver staining, $1200\times$

Fig. 5. Collaps of glomerular loops, undulation of BM, $5\frac{1}{2}$ months after transplantation (case 13). PAS, $440\times$

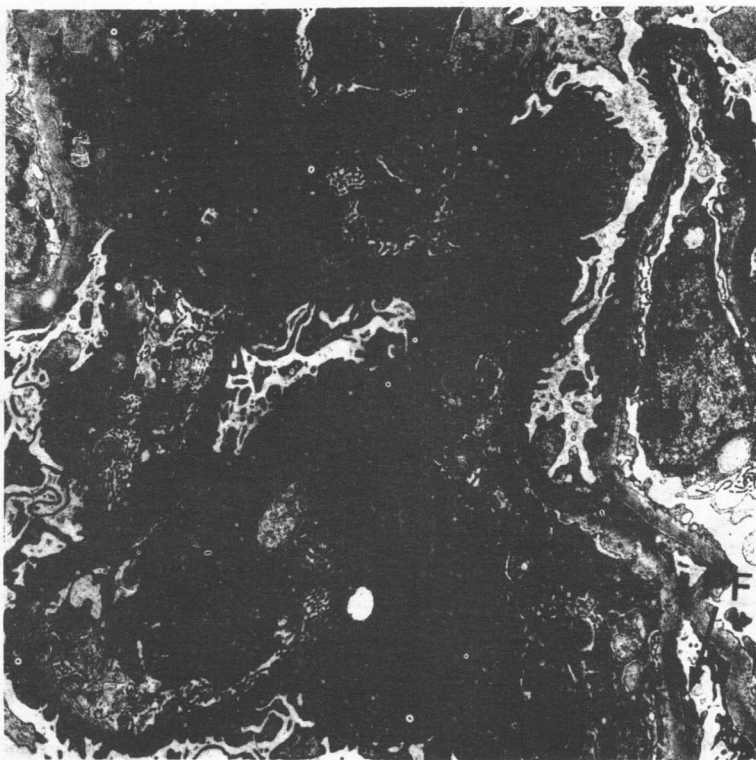


Fig. 6. Electronmicroscopic photograph of a typical TGP, 9 months after transplantation (case 20). Thickened BM. Garland-shaped arcades of endothelium (E) are almost completely the lumina of the loops. Basement membrane-like substance (B) of the mesangium much increased without multiplication of the nuclei, focal pedicle fusion (PF). 3570 \times

More frequently, cell constituents, consisting partly of cytoplasmic constituents, only enclosed by a membrane (Fig. 14), can be found in this thickened internal lamina rara; partly, however, genuine endothelial invaginations, extending into this loosened area, can be recognized (Fig. 15). At a very high degree of TGP these cell inclusions may become huge. Scattered mesangial cells seem to creep under the lamina densa into the region of the thickened lamina rara (Fig. 8). At subsequent phases, there are often osmiophilic finely granular structures of different shapes in the region of the intensely thickened internal lamina rara; this may cause obliteration of a loop. These deposits partly impress as coarse lumps (Fig. 15) which are characterized by a rather precise outline but no membrane.

Two of our cases show large osmiophilic subendothelial deposits, as can be found in lupus nephritis: case 1 with morbus Fabry, case 5 with chronic-interstitial non-destructive nephritis as primary disease (Fig. 16). 6 out of 12 patients with glomerulonephritis as primary disease showed smaller osmiophilic deposits at electron microscopy. The same applied to 4 out of 9 patients with other primary diseases (s. Table 1).

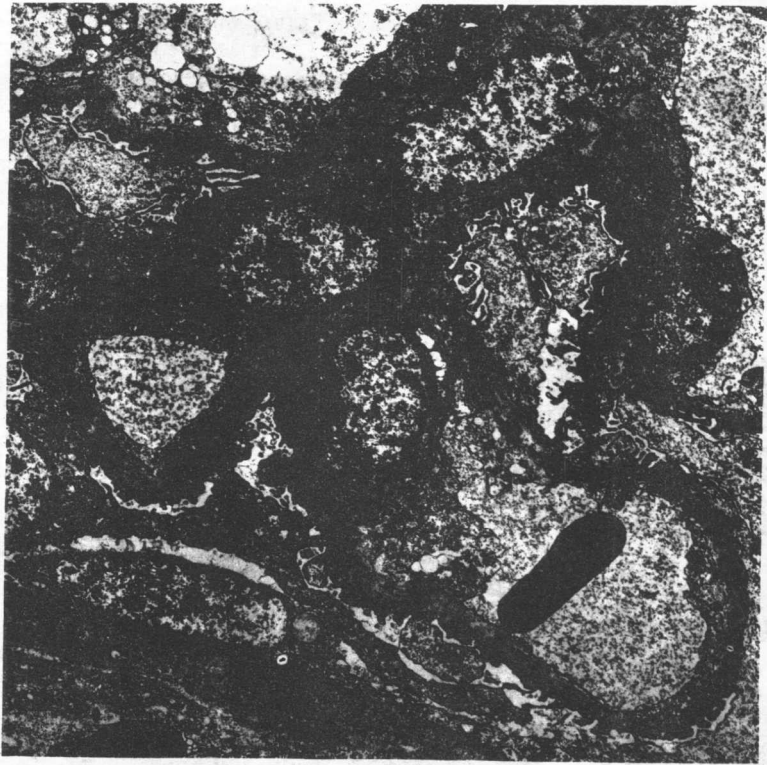


Fig. 7. Peripheral part of collapsed glomerulum, 14 months after transpl. (case 2). BM severely thickened and sporadically pleated. Mesangium not enlarged, endothelium unchanged. 3910 \times

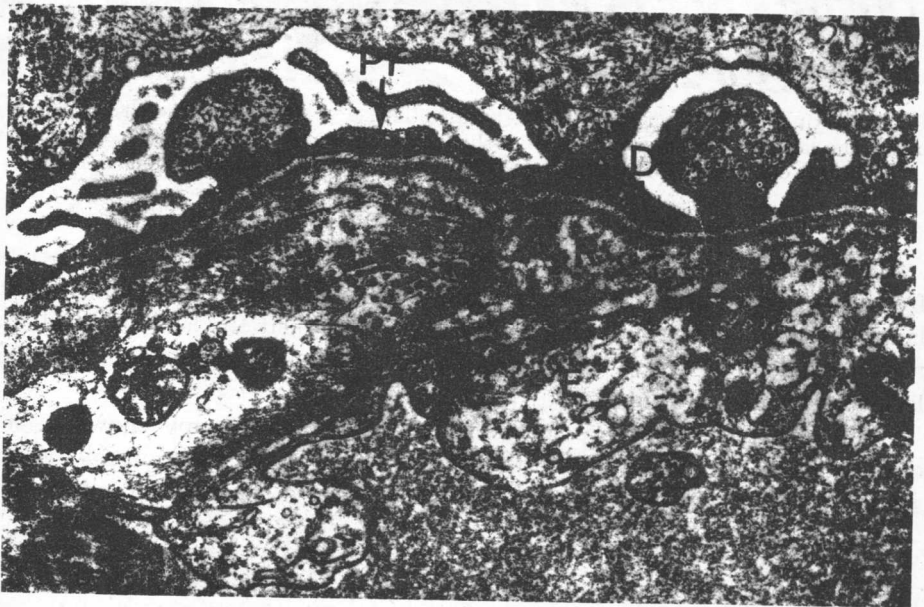


Fig. 8. Section of glomerular loop wall, 7 months after transpl. (case 20). BM as a whole thickened, lamina densa (D) rarified, lamina rara interna (R) electron-lucent, a mesangial cell is creeping into the lamina rara interna (\rightarrow). Endothelial cells (E) activated, visceral epithelial cells with hinted pedicel-fusion. 16900 \times

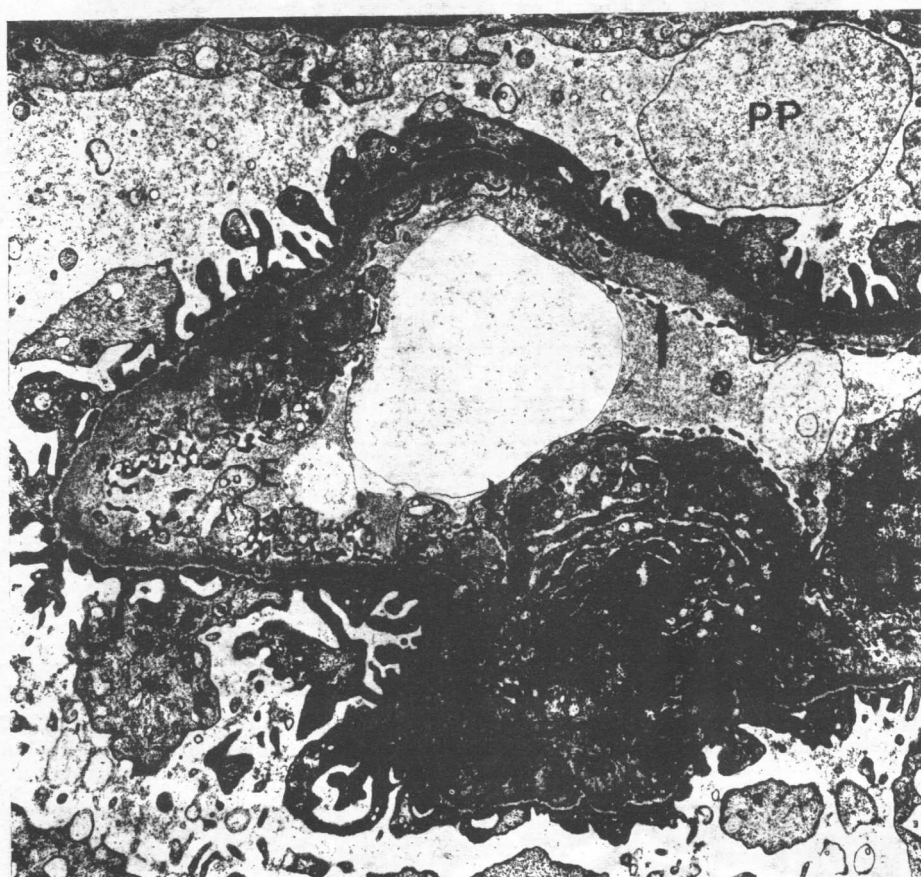


Fig. 9. Distinct TGP (+), 19 months after transpl. (case 5). Cushion-like localized thickening of the lamina rara interna (→), endothelium with arcade formation (E), processes of visceral epithelial cells edematous (PP). Only hinted pedicular fusion. 6300 ×

Osmiophilic, narrow bands under the endothelium can be differentiated from these deposits (Fig. 17); their optic density and structure reminds of the lamina densa. From this structure all kinds of transitions lead to parallel or netlike osmiophilic layers. In some cases, an osmiophilic, rather plump fibrillar lacework developed (Fig. 17).

In the extremely severe form of TGP, light microscopy shows a clear duplication of the BM in silver-stained sections (Fig. 4). Electron microscopic studies reveal a split-up, lamina densa-like structure beneath the endothelium

Fig. 10. Very slight TGP (\pm), 14 months after transpl. (case 2). *R* Small electron-lucent cushion of the lamina rara interna. *PP* Edematous processes of epithelial cells. *V* Vacuoles in endothelial cells. *X* Hyaline droplet in endothelial cell. 15600 ×

Fig. 11. Nodular protrusion (*P*) on the endothelial face of the BM, 30 days after transpl. (case 6). 18000 ×